EnvironmentAsia
The international journal published by the Thai Society of Higher Education Institutes on Environment

Available online at www.tshe.org/EA
EnvironmentAsia 6(2) (2013) 24-33

Radar Reflectivity Derived Rain-storm Characteristics over Northern Thailand

Pakdee Chantraket, Chanti Detyothin and Anuchit Suknarin

Department of Royal Rain-making and Agricultural Aviation (DRRAA) 50, Inside Kasetsart University, Ladyao, Chatuchak, Bangkok 10900, Thailand

Abstract

The radar data analysis in this study were to extract the radar reflectivity to individual rain-storms and present the study on rain-storm characteristics with their crucial features in northern Thailand over 80 days between April and August 2012. This study classified the two seasonal variations of rain-storm characteristics derived from Thunderstorm Identification and Tracking Analysis and Nowcasting (TITAN) algorithm including 11 variables of storm numbers, duration, volume, mass, sizes, maximum reflectivity and movement in the data set. Additionally, the study also evaluated statistically the relationship between storm characteristics and standard instability indices including lift index (LI) and convective available potential energy (CAPE).

It can be seen that in summer season had a smaller number of storms but the storms were of longer average duration, greater maximum reflectivity as well as larger areas, volume and mass. Most rain-storms in both summer and rainy seasons were less than 2 hours and the storm altitudes (base to top height) were between around 2 and 8 km MSL. The storm velocity was not exceeding 20 km/hr and their movement was southeasterly wind accordingly along the north-south mountain ranges in northern Thailand. Storm area was the most important factor determining the convective weather in the large scale environment during summer season since it was illustrated the strongest correlation in both LI (negative; -0.67) and CAPE (positive; 0.65). Alternatively, the storm duration was the most important variable in wet season, which was exhibited the strongest correlation (0.68) with CAPE as well; moreover, no such strong correlation was found for LI.

Keywords: Northern Thailand; TITAN; rain-storm; thunderstorms; weather radar; radar reflectivity; sounding data

1. Introduction

A convective storm is meteorological phenomena that are generated by the heating of the earth and with deep moisture. The convective storm accompanied by lightning and thunder and a variety of weather such as locally heavy rains leading to flash flooding, strong winds, sudden temperature changes, and in some cases hail (Doswell *et al*., 2000). In Thailand during rainy season, major flash flooding is often caused by heavy raining from severe convective weather. However, the convective rain-storm is still an important key to possible rain enhancement feasibility potential in order to relieve draught in summer season as well. For this reason the comprehension in convective weather structures and characteristics are leading to the basic of development in atmospheric water resources management in Thailand.

Nowadays, weather radar is widely used to detect the convective storms and study of convective storm structure due to its capability for spatial and temporal storm profiles measurement. Radar data-based storm characteristics studies appeared in the USA in the 1950s following the invention and first use of weather radars (Braham, 1958; Battan, 1963). Subsequently, there are many storm studies using weather radar e.g. Zipser *et al*., 1994; Toracinta *et al*., 2002. Goudenhoofdt *et al*., 2010 studied 5 years of convective storm characteristics data based on reflectivity measurement from weather radar in South-east Belgium in order to study storm evolution characteristic which aimed to improve its nowcasting. While, Potts *et al*. (2000) using radar echoes in Sydney, Australia to study 12 cases of active diurnal convection in the summer of 1995/96. Besides the result shown that both maximum reflectivity and storm height are correlated with the logarithm of storm volume, they also found out that even there were a number of small storms but the volume of precipitation flux are mostly contributed by few large-scale storms. Walther *et al*. (2006) used 3 years of weather radar data composites over the Baltic region to determine the criterion of distinguishing “frontal” and “convective” precipitation. Meanwhile in Thailand there are still a few studies in cloud and rain-storm characteristics using radar data. Rain-cloud studies using radar-based have been performed by Chumchean (2009), who investigated and classified rainfall event using rain-cloud horizontal characteristics obtained from radar reflectivity images with 2.5-km CAPPI (Constant altitude plan position indicator) from of Royal Rain-making and Agricultural Aviation (BRRAA)'s radar station at Pimai district, Nakhon Ratchasima during 2003-2005 in northeast Thailand.

The purpose of this paper is to present the study of rain-storm characteristics and identify the intraseasonal variation between summer and rainy seasons over northern Thailand. The important storm properties, structures and their behaviors are analyzed and the relationship between storm characteristics and standard instability indices are discussed (Cifelli, 2007). Radar reflectivity and sounding data were obtained from weather station of DRRAA which situated at omkoi district, Chiang Mai. The storm characteristics were run through the Thunderstorm Identification and Tracking Analysis and Nowcasting (TITAN) (Dixon *et al*., 1993) and standard instability indices were computed by using sounding data. These instrumentations can provide an efficient way to study and observe the storm characteristics as well as their essential features which derived from 80 days during April to August 2012. There were carried out over radar effective radius 240 km in the northern Thailand (Fig. 1).

2. Data Sets and Method

The data sets that were used in this study including (1) rain-storm characteristics obtained from radar reflectivity measurement and (2) instability indices computed by radiosonde observation. These data were chosen merely in a day of available completion both in radar and sounding data. Total data were selected for 80 days during 32 days in dry summer and 48 days in rainy season between Apr 2012 and Aug 2012 over northern Thailand.

RADAR: This study was used radar reflectivity-derived parameters from S-band Doppler radar with dual polarization (SIDPOL) which is operated by DRRAA. SIDPOL is situated in Omkoi district, Chiangmai, northern part of Thailand as shown in Fig. 1. This radar has collected the reflectivity data as volume scan to the highest altitude at 20 km provided in the universal format files (UF) (Barnes, 1980), which are obtained every 6-minute interval by using 15 elevation angles; 0.6^{O}, 1.4^{O}, 2.2^{O}, 3.1^{O}, 4.0^{O}, 4.8^{O}, 5.6^{O}, 6.5^{O}, 7.7^{O}, 9.1^{O}, 10.7^{O}, 12.6^{O}, 14.9^{O}, 17.5^{O} and 20.2^{O}, with the effective range of 240 km.

TITAN: The SIDPOL reflectivity data were run through the TITAN. The TITAN algorithm could objectively identify the storms, track the storm movements and analyze their properties as Table 1.

The storms were selected for this study's dataset form the following criteria as followed: (Dixon, 1998; Bampzelis *et al*., 2012)

1) Strom track within 240 km of the radar.
2) Reflectivity threshold 30 dBz or greater.
3) Minimum storm size as 10 km^2.
4) Using the Marshall-Palmer Z-R relationship applied to estimate precipitation in the storm.
5) The storm mass is computed using the Z-M relationship; $m=20300*Z^{1.67}$, where m is the water content in g/m^3 and Z is the radar reflectivity factor in mm^6/m^3.

Table 1 lists the 11-TITAN storm characteristics used in this study. The dataset contained 80 days during summer and rainy season 2012.

SOUNDING DATA: Soundings are routinely taken at weather observational station locating at Omkoi district, Chiangmai, Thailand (Fig. 1) during summer to late rainy season every year. Providing insight into the environment conditions within the Omkoi radar domain for each day, these indices compose of lifted index (LI) (Galway, 1956) and convective available potential energy (CAPE) (Moncrieff *et al*., 1976; Gettleman *et al*., 2002) were determined for the 0000UTC sounding.

Table 1 Radar-obtained storm characteristics from TITAN and their units

Rain-storm characteristics	Variables	Units
(1) Number of storms	NoS	Counts
(2) Storm duration	S_Dur	hrs
(3) Maximum volume	S_Vol	km^3
(4) Maximum mass	S_Mas	ktons
(5) Maximum envelope area	S_Area	km^2
(6) Maximum precipitation area	Precip_Area	km^2
(7) Maximum storm-top height	S_Top	km MSL
(8) Maximum storm-base	S_Base	km MSL
(9) Maximum reflectivity	S_dBz	dBZ
(10) Mean speed	S_Vel	km/hr
(11) Mean direction	S_Dir	deg

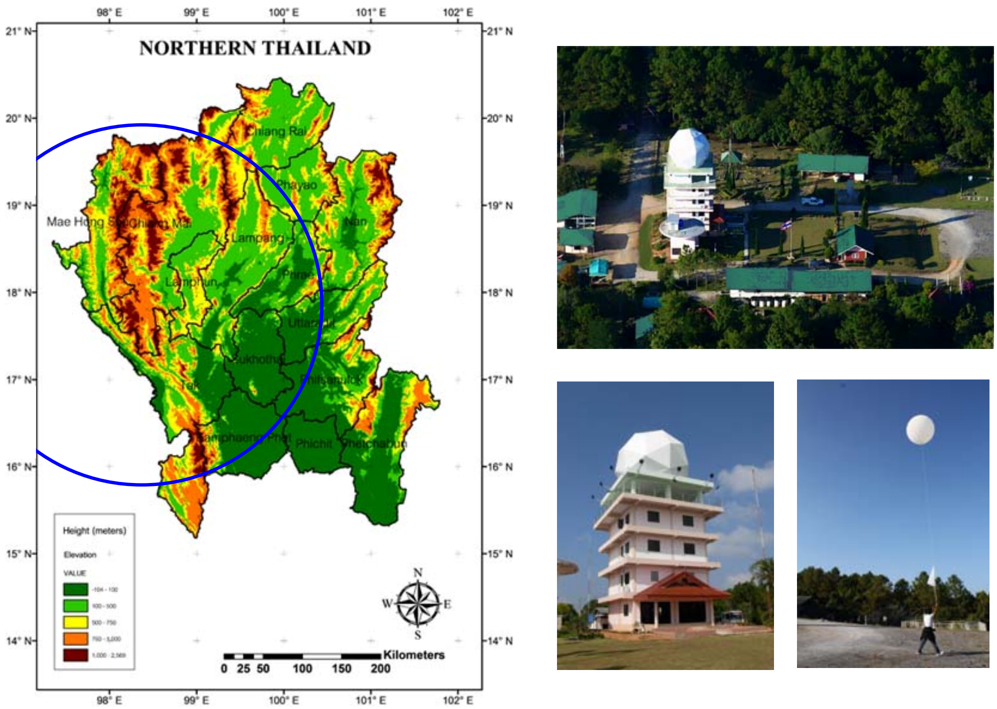

Figure 1. The study area in radar effective range 240 km over northern Thailand (18 00 N 100 00 E) and DRRAA observational weather station at Omkoi (18 47 54 N, 98 25 56E, 1163m MSL), Chiang Mai, Thailand.

The LI is computed by the determination of the lifted parcel pressure, temperature and dewponit. The parcel is assigned the mean mixing ratio of the lowest 50 mb as the formal definition is given by

LI = Temperature of Environment at 500 mb - Parcel temperature at 500 mb (1)

In contrast, to single level stability indices, CAPE is a vertically integrated index and measures the cumulative buoyant energy in the free convective layer (FCL) from the level of free convection (LFC) to the equilibrium level (EL) (David, 1998). The formal definition is given by

$$CAPE = g\int_{Z_{LFC}}^{Z_{EL}} \left(\frac{T_{Vp} - T_{ve}}{T_{ve}} \right) dz \qquad (2)$$

Where T_{vp} is the virtual temperature of the parcel and T_{ve} is the virtual temperature of the environment, Z_{EL} is the height of the equilibrium level, Z_{LFC} is the level of free convective, and g is gravity. The calculation CAPE (J/kg) was based on lifting a well-mixed parcel from lowest 50mb (mean temperature and mixing ratio).

3. Result

3.1. Characteristics of Rain-Storm

3.1.1. Rain-storm number and lifetime

The result and example from this study exhibits that an average number of storms were found in summertime is extremely smaller than in rainy season as indicated in Fig. 2 and 3, respectively. From daily individual

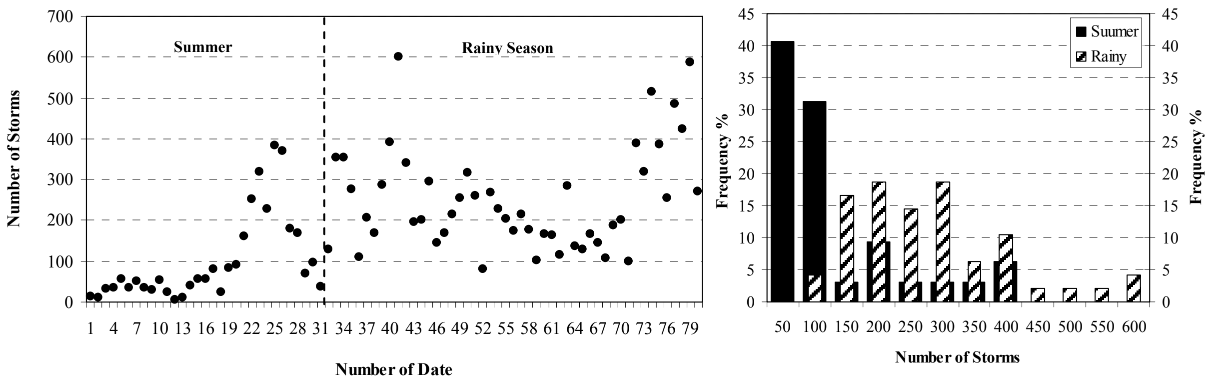

Figure 2. Show the number of storms (left) and frequency distribution (right) during summer and rainy season.

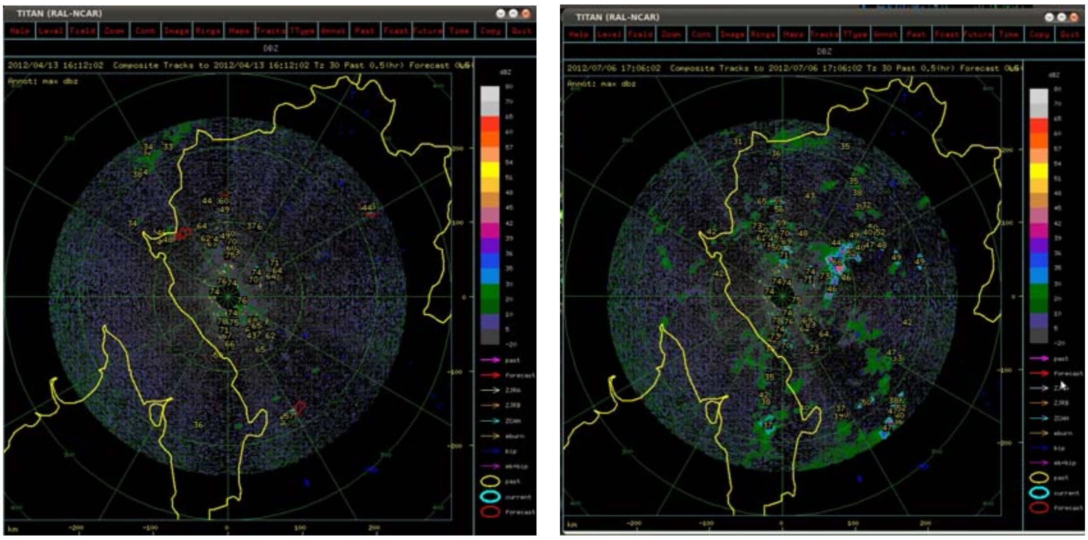

Figure 3. Some cases of rain-storm number from TITAN analysis: (a) April 13, 2012, 16:12:02 in summer season and (b) July 06, 2012, 17:06:02 in rainy season.

storm tracking is shown that the numbers of storms are between 6 and 384 in summer period but between 80 and 600 in rainy season.

As for storm duration is the time elapsed from the first radar echo of 30 dBz until the disappearance of precipitation. In this study revealed that the average individual storm duration during summertime was longer than in rainy season, around 1 hour in summer and 40 minutes in rainy season, respectively and almost all storm durations in both seasons were less than 2 hours. It is apparent that in summertime had a smaller number of storms but the storms were of longer average duration (0.5 to 2.0 hr) as well. The time series of storm duration on each season is illustrated in Fig. 4.

3.1.2. Rain-storm height

The storm bases and tops show the minimum and maximum height of radar reflectivity, respectively as determined threshold. In this study were setting up the minimum reflectivity threshold at 30 dBZ; therefore, the radar will only report those bases and tops that are at a reflectivity of 30 dBZ or higher. The results of this study showed that an average of echo bases and tops are quit similar in both seasons, about 2.0 to 7.3 km MSL in summer and about 2.3 to 7.6 km MSL in wet season. The seasonal variation of the storm bases and tops as shown in Fig. 5.

3.1.3. Rain-storm mass and volume

Regarding storm's volume and mass it is found that average maximum cell volume is around 254 km^3 in summer and 170 km^3 in wet season. In addition, an average-maximum cell mass is around 185 ktons in summer and smaller in wet season, 75 ktons. The additional information of statistical analysis is presented as Table 2 and Table 3.

The result from this study exhibits that the storm volume and mass in summertime is greater than in rainy season with up to about 30% and 60%, respectively. The variation of these properties along seasonal period is presented in Fig. 6.

3.1.4. Rain-storm reflectivity

The result from this study showed that on average

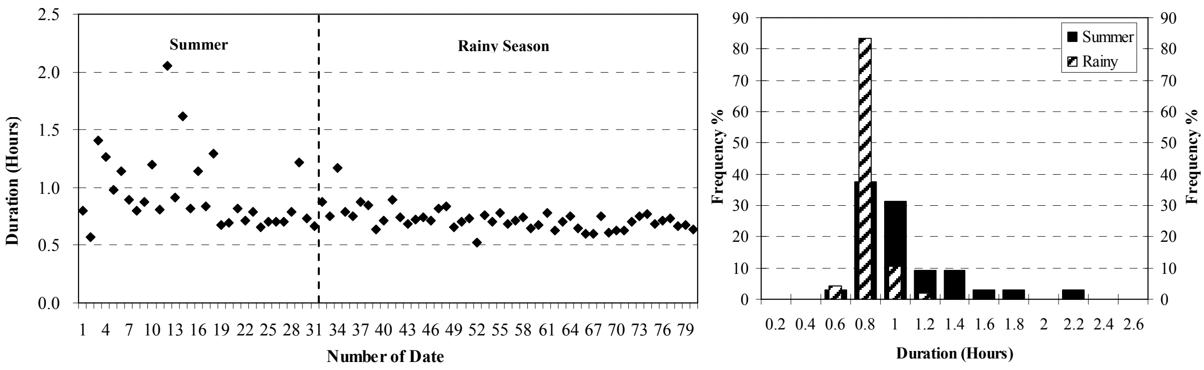

Figure 4. The average storm duration (hours) (left) and frequency distribution (right) during summer and rainy season.

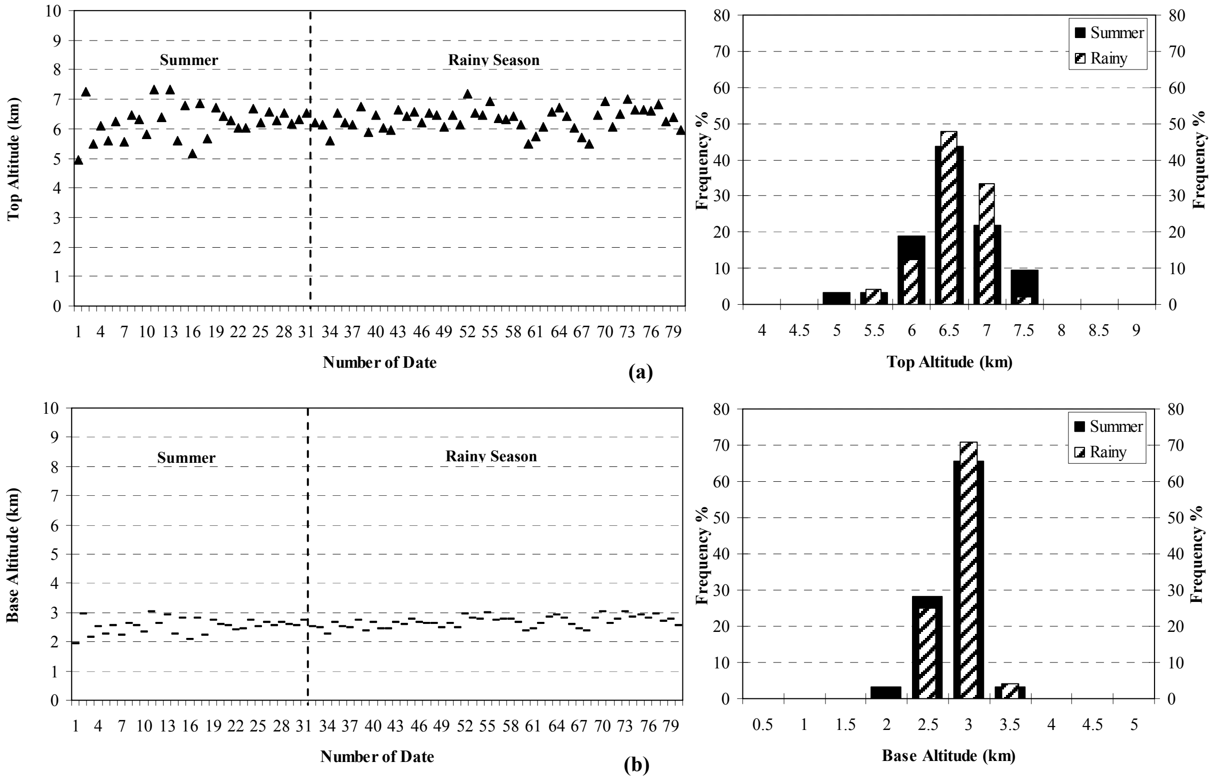

Figure 5. Show the average maximum storm (a) top (km MSL) and (b) base (km MSL) (left) and frequency distribution (right) during summer and rainy season.

Table 2. The storm characteristics during summer season 2012 over northern Thailand

Storm characteristics, LI and CAPE: Summer Season

	NoS	S_Dur	S_Vol	S_Mas	S_Area	Precip_ Area	S_Top	S_Base	S_dBz	S_Vel	S_Dir	LI	CAPE
	counts	hrs	km^3	ktons	km^2	km^2	km MSL	km MSL	dBZ	km/hr	deg	^oC	J/kg
Median	56.00	0.82	242.50	187.21	68.26	5.98	6.29	2.55	49.24	10.97	121.30	-1.83	2939.50
Mean	100.78	0.94	254.83	201.03	70.37	8.63	6.25	2.54	49.44	10.99	122.98	-1.70	3041.50
STD.	105.04	0.32	94.51	109.99	24.04	8.89	0.58	0.26	3.40	2.92	32.01	1.26	2017.08
Min	6.00	0.57	102.18	69.49	39.13	0.00	4.93	1.93	41.82	6.30	70.30	-3.85	202.00
Max	384.00	2.05	505.79	510.27	123.19	34.97	7.34	3.02	58.95	18.43	266.05	0.49	7819.00

Table 3. The storm characteristics during rainy season 2012 over northern Thailand

Storm characteristics, LI and CAPE: Rainy Season

	NoS	S_Dur	S_Vol	S_Mas	S_Area	Precip_ Area	S_Top	S_Base	S_dBz	S_Vel	S_Dir	LI	CAPE
	counts	hrs	km^3	ktons	km^2	km^2	km MSL	km MSL	dBZ	km/hr	deg	-	J/kg
Median	215.00	0.71	165.11	67.24	47.84	2.62	6.41	2.66	44.07	9.59	140.20	-0.27	306.00
Mean	252.71	0.72	172.07	75.44	48.29	3.06	6.33	2.67	44.10	10.64	149.86	-0.27	597.96
STD.	125.52	0.10	47.44	25.73	12.22	1.95	0.39	0.19	1.77	3.30	51.21	1.02	768.16
Min	81.00	0.53	93.63	32.32	24.52	0.40	5.47	2.25	38.37	6.50	69.24	-2.39	0.00
Max	600.00	1.17	310.39	150.56	85.71	10.84	7.17	3.04	48.13	19.07	262.83	2.03	4221.00

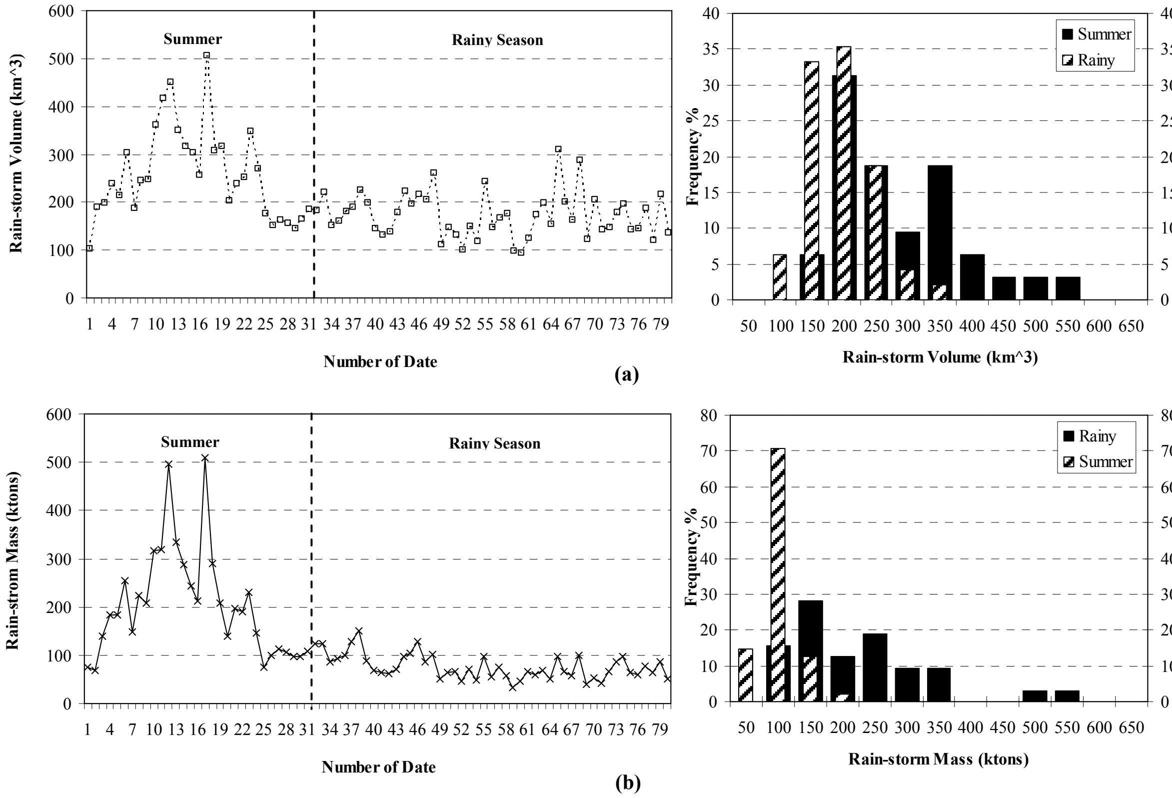

Figure 6. The average maximum value of (a) cell volume (km^3) and (b) mass (ktons) (left) and frequency distribution (right) during summer and rainy season.

maximum value, storm's reflectivity peaks that occurred during summer at about 50 dBz ranging between 42 and 59 dBz. However, the smaller reflectivity occurred during rainy season which was approximately to 44 dBz ranging between 38 and 52 dBz. The average maximum value of reflectivity was presented in Fig. 7.

3.1.5. Rain-storm area and precipitation area

Storm and rainy area of each season are distinguished between summer and rainy season. The larger average raining area from individual storm cell is shown in summer that is approximately 70 km^2 and, 48 km^2 in rainy season. Although the number of storms in summer is smaller comparing in wet season, summer rain-storm composes of several large cells, and they can lead to larger areas obviously. The average area of rain-storm was presented in Fig. 8.

3.1.6. Rain-storm movement

TITAN algorithm can provide the information of storm tracking and its movement. The results obtained from this study showed that the mean velocity and direction of summer rain-storm are 11 km/hr and 122 degree (ESE; 101.25 ^{o} -123.75^o), while in rainy season the value of average storm velocity and direction are 10 km/hr and 177 degree (S; 168.75 ^{o} -181.25 ^{o}). The average rain-storm movement in both seasons was illustrated in Fig. 9.

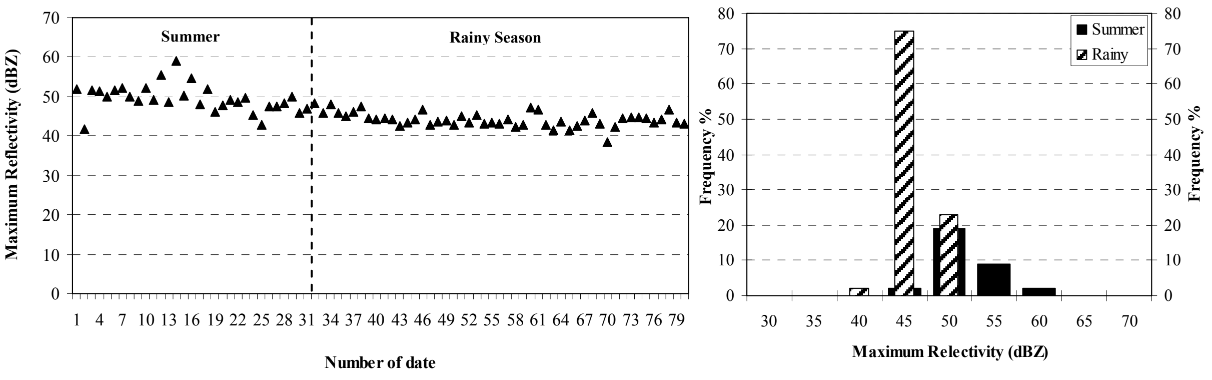

Figure 7. Show the mean value of maximum storm reflectivity (dBz) (left) and frequency distribution (right) during summer and rainy season.

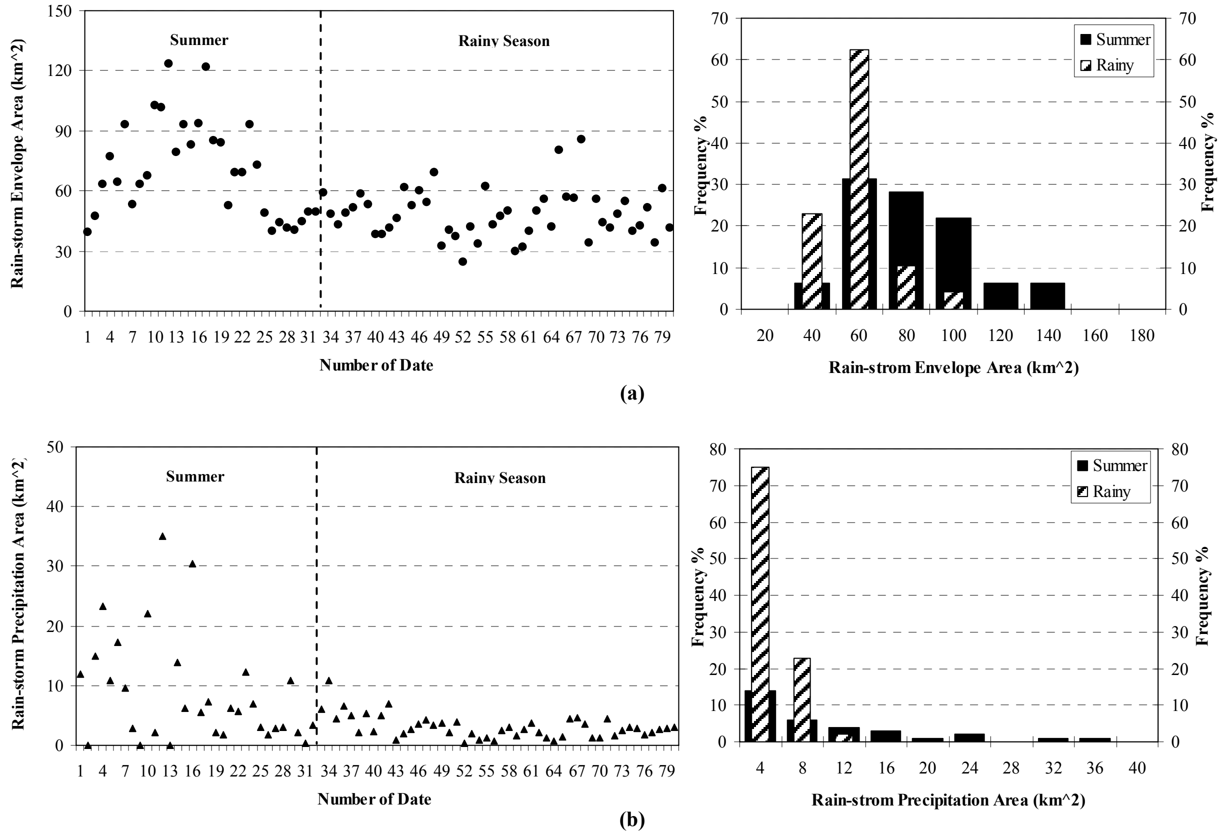

Figure 8. The mean value of (a) rain-storm area (km^2) and (b) precipitation area (km^2) (left) and frequency distribution (right) during summer and rainy season.

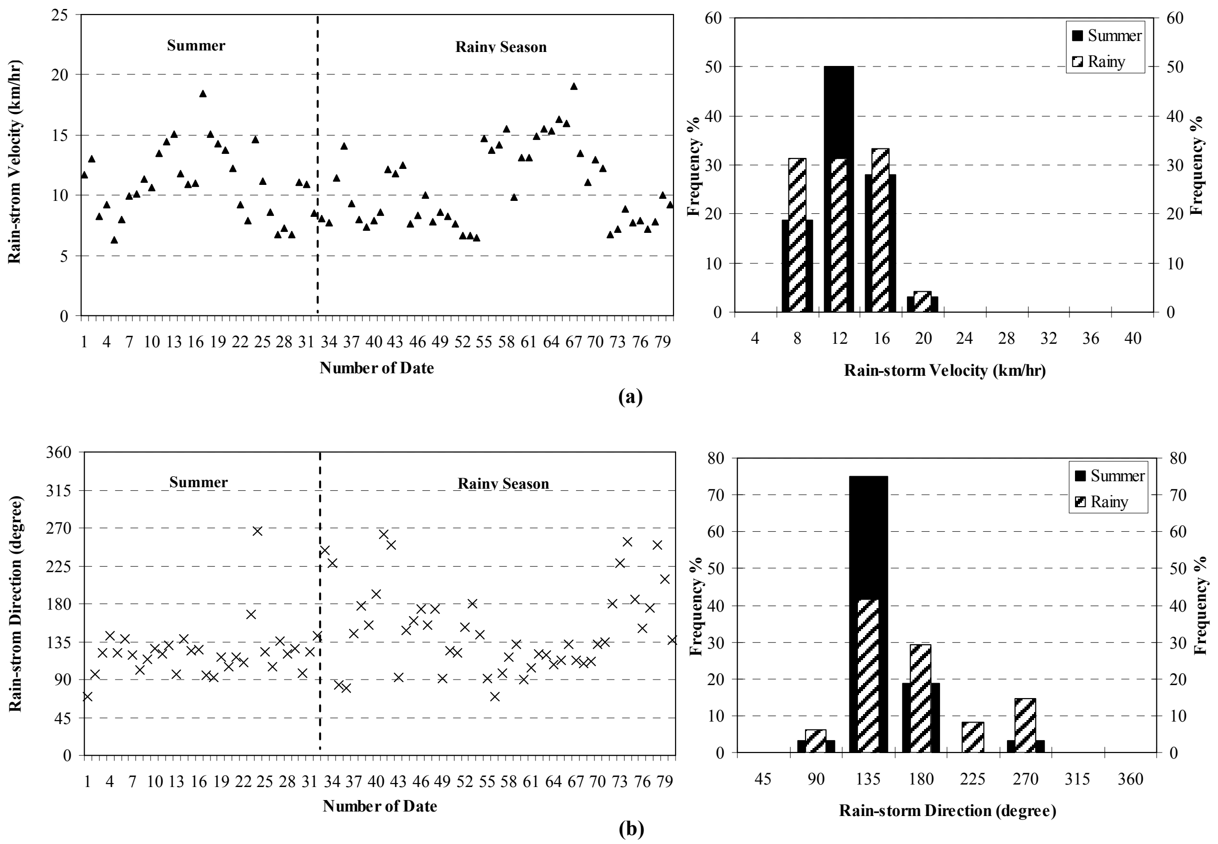

Figure 9. Show the mean value of rain-storm movement including mean (a) velocity (km/hr) and (b) direction (degree) (left) and frequency distribution (right) during summer and rainy season.

3.2. Assessing the Relationship between Thunderstorm Characteristics and Standard Instability Indices

The purpose of this study is to use sounding data to examine several parameters commonly used to forecast storm and severe weather. Then the chosen stability indices are designed specially to evaluate mostly in the convective and severe weather applied to rain-storm forecasting including LI and CAPE (Fig. 10). As the result, assessing the possible correlations of reflectivity feature with changes in the large scale environment, the rain-storms were interpolated to the upper air sounding station that is located in effective range of radar observation.

The statistical result in this study illustrated an average LI and CAPE (Table 2 and Table 3) occurring during summer at around -1.7 and 3000 J/kg and during wet season at around -0.27 and 600 J/kg. However from the frequency distribution, values of LI normally distributed about a mean of approximately ‘-2’ in summertime and ‘0’ in wet season, as indicated in Fig. 10(a). CAPE values are distributed close to 1000 J/kg in both season but they have a wider distribution around to 8000 J/kg in summer season, as indicated in Fig. 10(b). Accordingly, the higher negative in LI and the stronger CAPE value exhibited that in the summertime the storm occurrences have a tendency to stronger instability and more possible thunderstorm availability.

Pearson’s correlation coefficient between two variables is defined as the covariance of the two variables divided by the product of their standard deviations. The formula for the Pearson product moment correlation coefficient, r, is:

$$r = \frac{\sum (X-\bar{X})(Y-\bar{Y})}{\sqrt{\sum (X-\bar{X})^2 \sum (Y-\bar{Y})^2}} \qquad (3)$$

Where x and y are the sample of two variable

For the Pearson’s linear product moment correlation coefficient analysis were shown that the relationships between rain-storm characteristics and stability indices by classified into two periods during summer and rainy season as illustrated in Table 4. The result obtained from this study showed as followed.

1) The strong correlation (|r|>=0.5) between rain-storm characteristics and LI was obtained from TITAN including maximum volume, maximum mass and maximum envelope area in summer while in rainy season all characteristics were a smaller correlation. The strongest correlation (-0.67) was shown relationships between maximum envelope area and LI in summer season.

2) As the strong correlation during summertime between rain-storm characteristics and CAPE including maximum volume, maximum mass, maximum

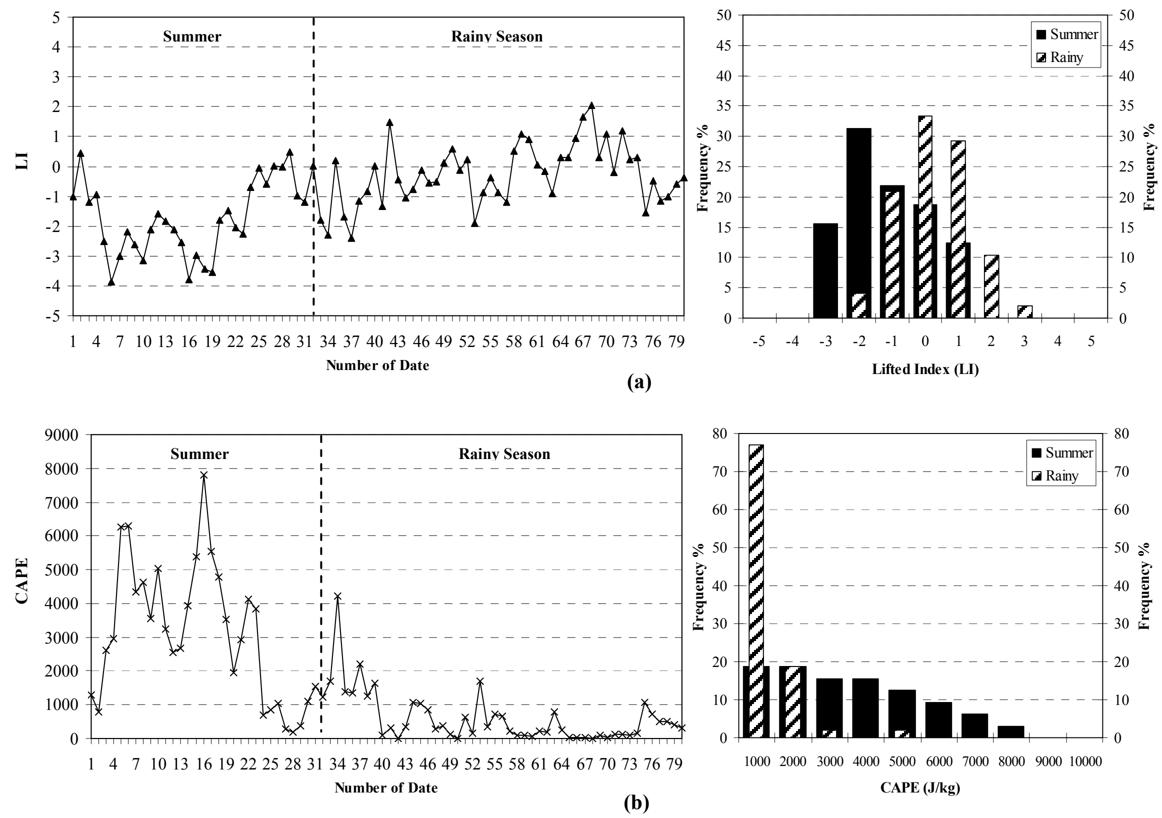

Figure 10. Time series of LI (a) and CAPE (J/kg) (b) derived from sounding (left) and frequency distribution (right) during summer and rainy season.

Table 4. LI and CAPE and rain-storm characteristic product moment correlation coefficient

Pearson's r N(SS)=32, N(RS)=48	LI		CAPE	
	SS	RS	SS	RS
(1) NoS	0.34	-0.27	-0.33	0.13
(2) S_Dur	-0.22	-0.48	0.28	***0.68***
(3) S_Vol	-0.58	-0.03	0.52	0.09
(4) S_Mas	-0.58	-0.39	0.55	0.47
(5) S_Area	***-0.67***	0.04	***0.65***	0.09
(6) Precip_Area	-0.30	-0.23	0.43	0.57
(7) S_Top	0.23	-0.12	-0.29	-0.15
(8) S_Base	0.24	0.02	-0.30	-0.30
(9) S_dBz	-0.47	-0.31	0.52	0.52
(10) S_Vel	-0.29	0.37	0.10	-0.29
(11) S_Dir	0.11	-0.24	-0.10	0.22

SS = Summer season, RS=Rainy season

reflectivity and maximum envelope area and including storm duration, maximum reflectivity and maximum precipitation area in rainy season, respectively. The strongest correlation (0.68) was shown relationships between storm duration and CAPE in rainy season.

4. Conclusions

In this study has examined statically the intraseasonal variations of essentially 11-storms characteristics obtained from TITAN including storm numbers, duration, volume, mass, sizes, reflectivity and movement in the data set. Frequency distribution of storm characteristics indicated their extensions and limitations, providing an integrated view of storm behavior over the examined area. It is relevant that in summer season (Table 2 and Table 3) almost storm characteristics had greater values of storm duration, volume, mass, areas and maximum reflectivity than in rainy season. During the time that in wet season, the number of storms is greater than double in summer period.

The other storm properties including storm altitudes (base to top height) and their movement are quite similar in both seasons. Most rain-storms had the storm altitudes between around 2 and 8 km MSL from base to top. The storm velocity was not exceeding 20 km/hr and their movement was southeasterly wind consistent along the north-south mountain ranges in northern Thailand.

The relationship between these storm characteristics and the chosen stability indices derived from sounding data consist of LI and CAPE (J/kg) were exhibited that the strongest negative correlation (-0.67) was shown relationships between LI and storm area in summer season but all characteristics were a smaller correlation in rainy season. The strongest positive correlation (0.68) was shown relationships between CAPE and storm duration in rainy season and there are a number of stronger correlation than LI. Consistently with previous study, these results confirm those of Blanchard (1998), Mackeen *et al*. (1999) and Derubertis (2006) who point out the correlation among storm characteristics, CAPE and LI in the United States respectively for thunderstorms. Consequently in both season, the CAPE is appropriately stability index which is applied to forecast the convective and severe weather changes in the large scale environment.

Acknowledgements

The authors gratefully acknowledge the Bureau of Royal Rainmaking and Agricultural Aviation (BRRAA), Bangkok Thailand for funding support through BRRAA research project 2012: forecasting model development using upper atmospheric weather observation in northern Thailand. We also appreciate the Research Group and the Royal-Rainmaking Atmospheric Observation Group for much helpfulness and providing the radar data sets and weather observation data used in this study.

References

Bampzelis D, Karacostas T. Radar Derived Storm Characteristics over Central Greece. Advances in Meteorology, Climatology and Atmospheric Physics, Springer Atmospheric Sciences 2012; 27-33.

Barnes SL. Report on a meeting to establish a common Doppler radar exchange format. Bulletin of the American Meteorological Society 1980; 61:1401-04.

Battan LJ, Relationship between cloud base and initial echo. Journal of Applied Meteorology 1963, 2: 333-36.

Blanchard OD. Assessing the Vertical Distribution of Convective Available Potential Energy. Weather and Forecasting (American Meteorological Society) 1998; 13: 870-77.

Braham RR, Cumulus cloud precipitation as revealed by RADAR-ARIZONA 1955. Journal of Meteorology 1958; 15: 75-83.

Chumchean S, Aungsuratana P, Khommuang A, Hanchoowong R. Study of Rain-Cloud Characteristics Using Weather Radar Data. 18th World IMACS / MODSIM Congress 2009; 3682-89.

Cifelli R, Nesbitt SW, Petersen WA, Rutledge SA, Yuter S. Radar Characteristics of Precipitation Features in the EPIC and TEPPS Regions of the East Pacific. Monthly Weather Review 2007; 135: 1576-95.

David OB. Assessing the vertical distribution of convective available potential energy. Weather and Forecasting 1998; 13: 870-77.

Dixon M, Wiener G. TITAN: Thunderstorm Identification, Tracking, Analysis, and Nowcasting—A radar-based methodology. Journal of Atmospheric and Oceanic Technology. 1993; 10: 785-979.

Derubertis D. Recent Trends in Four Common Stability Indices Derived from U.S. Radiosonde Observations. Journal of Climate 2006; 19: 309-23.

Dixon M. Report on Preliminary radar based analysis of seeding effects. Coahuila Rainfall Argumentation Program 1997/1998 Seasons, NCAR, USA. 1998; 1-7.

Doswell, Charles A. Severe Convective Storms—An Overview. Meteorological Monographs 2000; 28: 1-26.

Galway JG. The lifted index as a predictor of latent instability. Bulletin of the American Meteorological Society 1956; 37: 528-29.

Gettelman A, Seidel DJ, Wheeler MC, Ross RJ. Multidecadal trends in tropical convective available potential energy. Journal of Geophysical Research 2002; 107: ACL17-1–ACL 17-8.

Goudenhoofdt E, Maarten R, Laurent D. Long term analysis of convective storm tracks based on C-band radar reflectivity measurements, ERAD 2010 – The sixth European conference on radar in meteorology and hydrology 2010.

Louis JB. Relationship between cloud base and initial radar echo. Journal of Applied Meteorology 1963; 2: 333-36.

Mackeen PL, Brooks HE, Elmore KL. Radar Reflectivity–Derived Thunderstorm Parameters Applied to Storm Longevity Forecasting. Weather and Forecasting (American Meteorological Society) 1999; 14: 289-95.

Moncrieff MW, Miller MJ. The dynamics and simulation of tropical cumulonimbus and squall lines. Quarterly Journal of the Royal Meteorological Society 1976; 102: 373-94.

Potts RJ, Keenan TD, May PT. Radar Characteristics of Storms in the Sydney Area. Monthly Weather Review 2000; 128: 3308-19.

Roscoe RB. Cumulus cloud precipitation as revealed by radar-Arizona 1955. Journal of Meteorology 1958; 15: 75-83.

Toracinta ER, Daniel JC, Eward JZ, Stephen WN. Radar, Passive Microwave, and Lightning Characteristics of Precipitating Systems in the Tropics. Monthly Weather Review 2002; 130: 802-24.

Vivekanandan J, Zrnic DS, Ellis SM, Oye R, Ryzhkov AV, Straka J. Cloud Microphysics Retrieval Using S-Band Dual-Polarization Radar Measurements. Bulletin of the American Meteorological Society 1999; 80: 381-88.

Walther A, Bennartz R. Radar-based precipitation type analysis in the Baltic area. Tellus A 2006; 58: 331-43.

Zipser EJ, and Kurt RL. The Vertical Profile of Radar Reflectivity of Convective Cells: A Strong Indicator of Storm Intensity and Lightning Probability. Monthly Weather Review 1994; 122: 1751-59.

Received 4 March 2013
Accepted 23 May 2013

Correspondence to
Pakdee Chantraket
Department of Royal Rain-making and Agricultural Aviation (DRRAA)
50, Inside Kasetsart University,
Ladyao, Chatuchak,
Bangkok 10900,
Thailand
Tel: 66-8618-1825
E-mail: pakdee2@hotmail.com